NANO LETTERS

pubs.acs.org/NanoLett Letter

Monitoring Plant Health with Near-Infrared Fluorescent H_2O_2 Nanosensors

Honghong Wu,[‖] Robert Nißler,[‖] Victoria Morris, Niklas Herrmann, Peiguang Hu, Su-Ji Jeon, Sebastian Kruss,* and Juan Pablo Giraldo*

Cite This: *Nano Lett.* 2020, 20, 2432−2442 Read Online

ACCESS | Metrics & More | Article Recommendations | Supporting Information

ABSTRACT: Near-infrared (nIR) fluorescent single-walled carbon nanotubes (SWCNTs) were designed and interfaced with leaves of *Arabidopsis thaliana* plants to report hydrogen peroxide (H_2O_2), a key signaling molecule associated with the onset of plant stress. The sensor nIR fluorescence response (>900 nm) is quenched by H_2O_2 with selectivity against other stress-associated signaling molecules and within the plant physiological range (10−100 H_2O_2 μM). *In vivo* remote nIR imaging of H_2O_2 sensors enabled optical monitoring of plant health in response to stresses including UV-B light (−11%), high light (−6%), and a pathogen-related peptide (flg22) (−10%), but not mechanical leaf wounding (<3%). The sensor's high biocompatibility was reflected on similar leaf cell death (<5%) and photosynthetic rates to controls without SWCNT. These optical nanosensors report early signs of stress and will improve our understanding of plant stress communication, provide novel tools for precision agriculture, and optimize the use of agrochemicals in the environment.

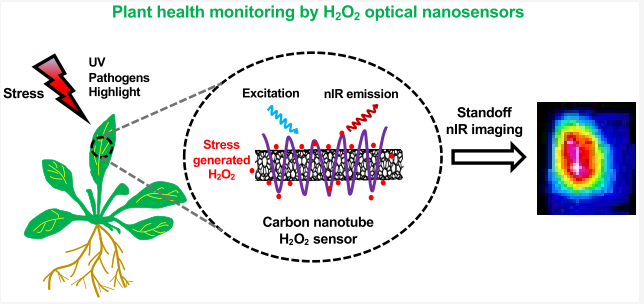

KEYWORDS: *Sensors, carbon nanotubes, plant stress, reactive oxygen species, agriculture, environmental nanotechnology*

Increased growth in the human population will require more than doubling food production[1]. This effort is impaired by a rapidly changing climate, exacerbating the frequency and intensity of environmental stresses and pathogen infections that negatively impact crop health and yield.[2−11] Precision agriculture aims to monitor crops for early detection of stress using sensors and autonomous and manned vehicles. However, these remote sensing instruments measure external environmental conditions or plant traits that often reveal stress after crops have begun to experience associated detrimental effects, including photosynthesis and chlorophyll content decline, and alone have limited potential of identifying the type of stress.[12,13] Plant phenotyping efforts identify traits that increase crop tolerance to environmental stress and disease and rely on plant structural, performance, or physiological parameters, but there are fewer tools available for monitoring plant's internal chemical signals associated with stress.[14−16]

Nanotechnology-based sensors are emerging tools for early detection of plant stress by enabling real-time monitoring of plant health via electronic devices.[17] Optical nanosensors have been demonstrated to report plant signaling molecules that communicate and trigger plant stress responses through epifluorescence microscopy of H_2O_2 and nitric oxide (NO) in leaf sections and remote detection of glucose in algae and whole plants.[18−20] Accumulation of reactive oxygen species (ROS) such as H_2O_2 is a hallmark of plant responses to stress.[21,22] Generation and accumulation of plant H_2O_2 have been reported in plants under most stresses including light stress, heat, salinity, wounding, and pathogen infection.[15,23,24] However, there are currently no H_2O_2 nanotechnology-based sensors able to respond to H_2O_2 in the plant physiological range from 10 to 100 μM.[17] Previous studies have demonstrated that single-walled carbon nanotubes (SWCNTs) are promising tools for biosensing applications.[25,26] Semiconducting SWCNTs display a chirality-dependent fluorescence in the near-infrared (nIR).[27] Different chemical functionalization approaches with nucleic acids, peptides, lipids, and proteins have been applied to tailor SWCNT surface chemistry.[28−31] These functionalized SWCNTs are highly sensitive to important molecules such as neurotransmitters (dopamine, serotonin), proteins, and nucleic acids.[32−36] It has been also known that nIR fluorescent SWCNTs coated with single-stranded DNA (deoxyribonucleic acid) (ss$(GT)_{15}$) report exogenously applied H_2O_2 from leaf sections at a concentration of 100 μM.[19] These studies were performed using custom-made nIR fluorescence microscopes under laboratory conditions. Similar sensors have also been

Received: December 15, 2019
Revised: February 14, 2020
Published: February 25, 2020

https://dx.doi.org/10.1021/acs.nanolett.9b05159
Nano Lett. 2020, 20, 2432−2442

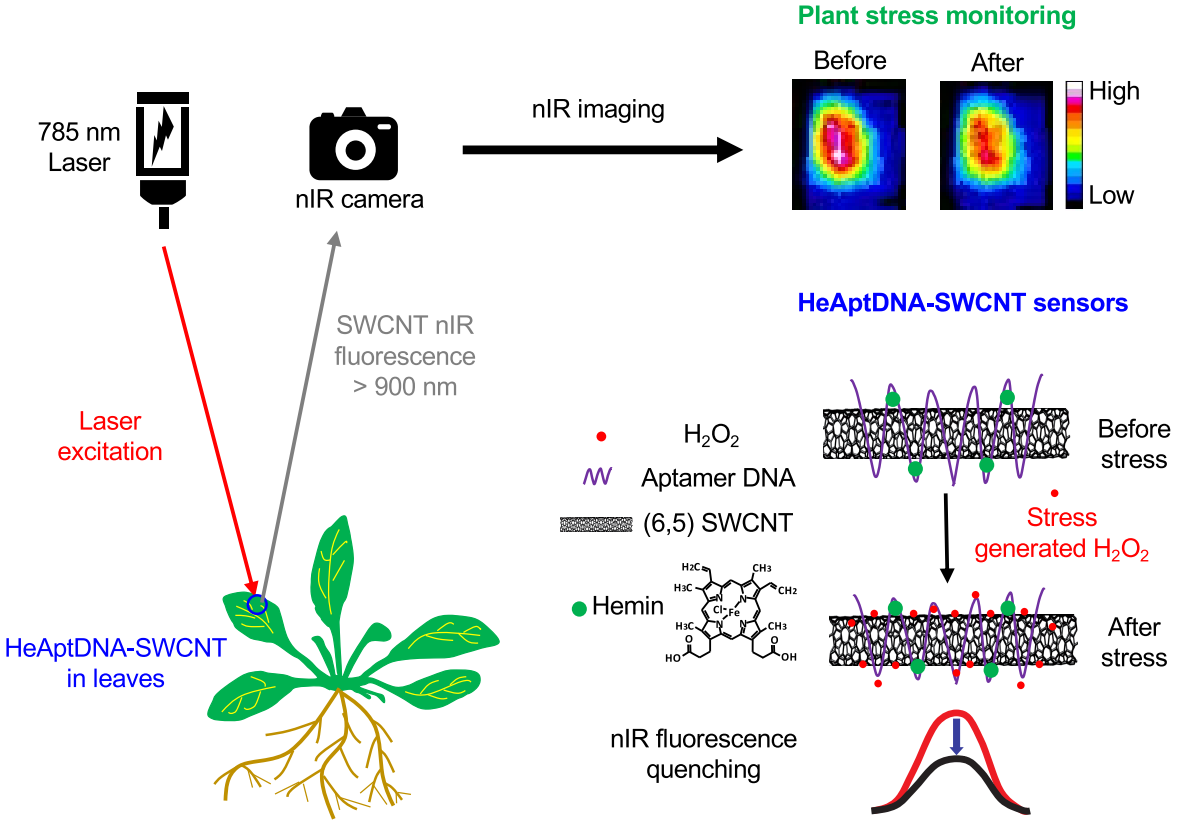

Figure 1. *In vivo* monitoring of plant health by SWCNT sensors for H_2O_2. SWCNTs functionalized with a DNA aptamer that binds to hemin (HeAptDNA-SWCNT) quench their nIR fluorescence upon interaction with H_2O_2 generated by the onset of plant stress. The spatial and temporal changes in nIR fluorescence intensity in leaves embedded with HeAptDNA-SWCNT sensors are remotely recorded by a nIR camera to assess plant health status.

shown to detect H_2O_2 molecules released from mammalian cells in real-time.[37,38] Optical nanosensors that signal the onset and type of stress to agricultural and phenotyping nIR imaging devices could indicate where and when improvement on plant growing conditions is needed, provide new monitoring tools for environmental stress and disease, and allow rapid screening of key plant chemical traits promoting stress tolerance. Because H_2O_2 is an excellent indicator for plant stress levels, the ability to monitor whole-leaf signaling molecule levels in mature plants could be very valuable for large-scale phenotyping purposes.[14,15]

Currently, we lack the ability to use noncontact electronic devices for remote monitoring of signaling molecules (e.g., H_2O_2) in wild-type plant species that remain difficult to genetically transform. Existing approaches to monitor plant H_2O_2 are based on genetically encoded sensors expressed in transgenic lines of plant model systems[39] that are not easily translatable to crops. Recently, fluorescent dyes for ROS detection were shown to report these signaling molecules to phenotyping devices such as Lumina S5 enclosed imaging systems under environmental and pathogen stresses.[15] Although it is an exciting application, fluorescent dyes photobleach and lack the signal-to-noise ratios to be detected by hyperspectral imaging cameras or portable devices, like smartphones, for applications in growth chambers, greenhouses, or the field. By contrast, SWCNT-based sensors do not photobleach and provide a temporal resolution adequate to detect plant stress responses and associated signaling molecules (H_2O_2) in both short- and long-term, from milliseconds to months.[17] These nanosensors have been reported to detect single molecules *in vitro*,[37] and their spatial resolution is only limited by the Abbe-limit, which allows localization of biomolecule generation sites at subcellular resolution.[40] SWCNTs are reversible sensors with long lifetimes that fluoresce in a region of the nIR spectrum where living tissues are relatively transparent.[41] We have previously used these water-soluble, nontoxic synthetic sensors in model and nontraditional plant systems[18,42] and demonstrated the crucial capability to monitor H_2O_2 in real-time in leaf sections of *Arabidopsis* plants.[19] However, the existing sensing approaches do not provide the necessary sensitivity that would enable remote H_2O_2 detection from living whole plants.[37,38]

Herein, we developed a H_2O_2 sensor based on SWCNTs functionalized with a DNA aptamer that binds to hemin (HeAptDNA-SWCNT) and allows remote monitoring of plant health and detection of both environment- and pathogen-related stresses. For accomplishing this goal we: (1) performed *in vitro* optimization of HeAptDNA-SWCNT detection of H_2O_2 within the plant physiological range (10−100 μM); (2) characterized the *in vivo* response of nanosensors to H_2O_2 in plant leaves; (3) assessed the biocompatibility of the nanosensors in plants; and (4) tested their performance in remote monitoring of plant stresses including UV-B, high light, wounding, and pathogen-related peptide (flg22). The newly developed HeAptDNA-SWCNT nIR sensors report H_2O_2 *in vivo* with a sensitivity and selectivity that enables the detection

https://dx.doi.org/10.1021/acs.nanolett.9b05159
Nano Lett. 2020, 20, 2432−2442

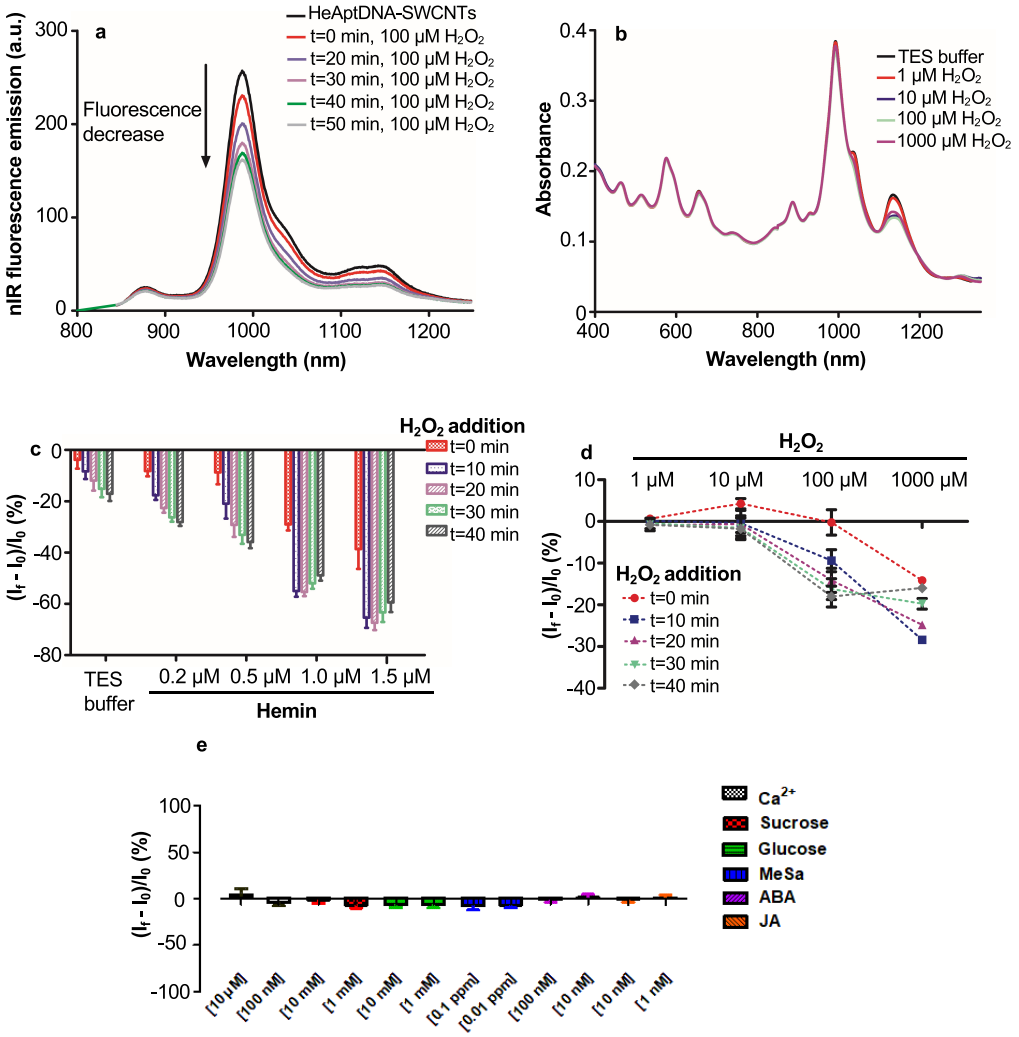

Figure 2. *In vitro* characterization of nIR HeAptDNA-SWCNT fluorescence response to H_2O_2. (a) nIR fluorescence emission of HeAptDNA-SWCNT sensors strongly decreases within 40 min after addition of H_2O_2 (100 μM). (b) Absorption spectra of HeAptDNA-SWCNTs (2 nM) with hemin (0.5 μM) 24 h after H_2O_2 addition of varying concentrations [1−1000 μM] indicate high colloidal stability. (c) Quantification of the optimal hemin concentration in HeAptDNA-SWCNTs (2 nM) to maximize the fluorescence response of sensors to 100 μM H_2O_2. (d) Fluorescence response of HeAptDNA-SWCNT to different H_2O_2 concentrations at the optimal hemin concentration of 0.5 μM. (e) Sensor nIR-fluorescence responses were below 10% $(I_f - I_0)/I_0$ for stress-associated plant ions, sugars, and hormones (Ca^{2+}, sucrose, glucose, methyl salicylate, abscisic acid, jasmonate); mean + SD (n = 3).

of the onset of plant stress using nIR imaging devices that are already utilized for precision agriculture applications.

Results and Discussion. *In Vitro HeAptDNA-SWCNT Sensor Response to H_2O_2.* To design a highly sensitive nIR reporter of H_2O_2 for monitoring plant health, we used SWCNTs as backbone and noncovalently functionalized it with an aptamer sequence (5′- AGTGTGAA ATATCTAAAC-TAAATGTGGAGGGTGGGACGGGAAGAAGTT-TATTTTTCACACT-3′) that binds to porphyrins[43,44] (Figure 1). This approach enabled the specific binding of hemin, a protoporphyrin IX complex that binds ferric iron (Fe^{3+}), which is known to undergo a Fenton-like reaction with H_2O_2 producing hydroxyl radicals.[38,45−47] SWCNTs have been reported to quench their nIR fluorescence in response to ROS.[38] However, previously published ss$(GT)_{15}$ coated SWCNTs sensors[19] could not achieve the desired sensitivity within the plant physiological range of <100 μM. Therefore, we tested hemin coated HeAptDNA-SWCNT in which H_2O_2 reacts to hydroxyl radicals, resulting in SWCNT fluorescence quenching. The HeAptDNA-SWCNTs exhibited a strong fluorescence quenching up to 50 min after H_2O_2 addition (Figure 2a). The characteristic SWCNT absorbance peaks were preserved for most chiralities in the presence of H_2O_2 at a range of concentrations from 1 to 1000 μM, indicating high long-term colloidal stability (Figure 2b). However, in the presence of H_2O_2, the absorbance of larger SWCNT chiralities, for example, (12,1), (8,4), (9,4), (8,4), (10,3), or (8,6)-SWCNTs decreased (Figures 2b and S1). Therefore, (6,5)-chirality enriched SWCNTs were used as a building block for sensing in biological experiments. The absorption spectra of these HeAptDNA-SWCNT show the presence of minor fractions of (6,4), (8,3), (7,5), (8,4), and (9,4) SWCNTs. Similarly, the two-dimensional (2D) excitation−emission spectra of HeAptDNA-SWCNTs indicate the most prominent nIR emission from the (6,5) chirality, followed by (7,5), (8,3), and (6,4)-SWCNT chiralities with lower nIR intensity (Figure S2). The number of bound aptamer-DNA was determined to be approximately 1 per 2.5 nm of SWCNT length (around 240

https://dx.doi.org/10.1021/acs.nanolett.9b05159
Nano Lett. 2020, 20, 2432−2442

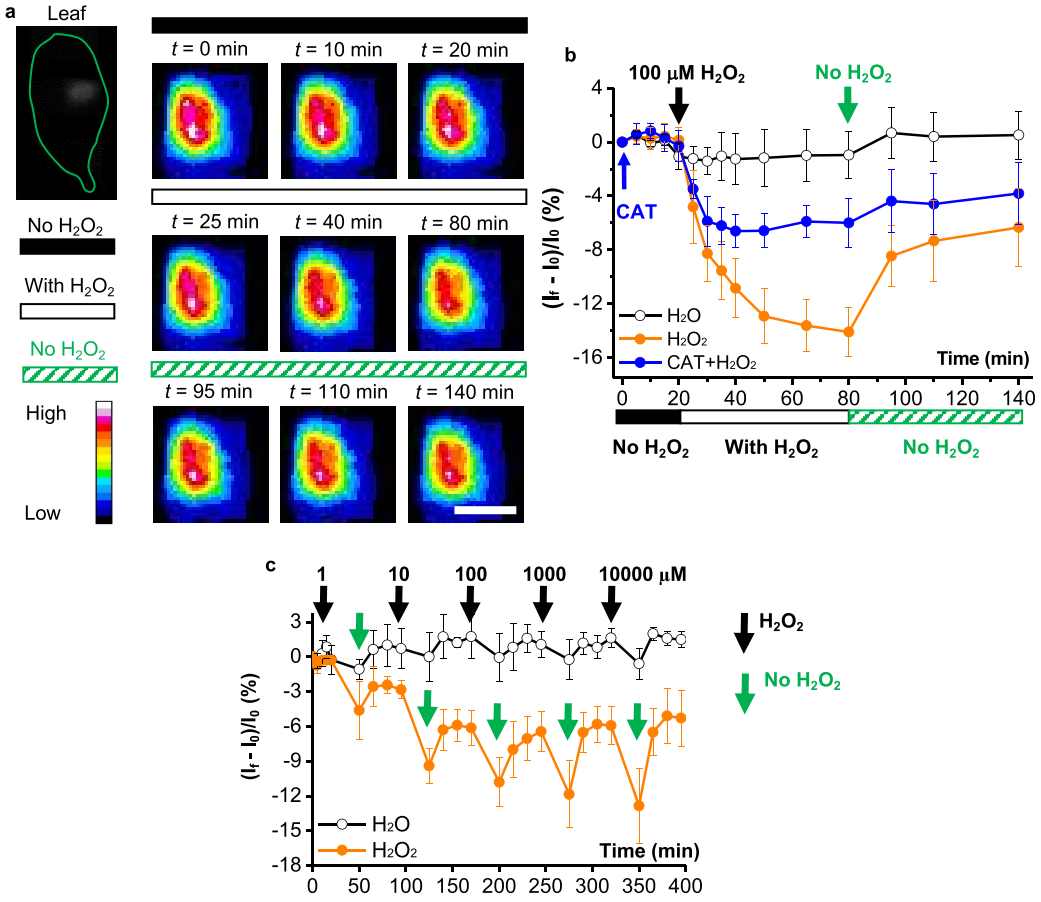

Figure 3. *In vivo* sensing of H_2O_2 by HeAptDNA-SWCNT in plant leaves. (a) nIR fluorescence images of HeAptDNA-SWCNT sensors embedded within *Arabidopsis* leaves and (b) corresponding nIR intensity changes in response to 100 μM H_2O_2 added topically on the leaf surface. Sensor fluorescence emission quenches upon exposure to H_2O_2, followed by partial recovery and stabilization of the fluorescence signal under the absence of H_2O_2. A H_2O_2 scavenging treatment of adding catalase (1500 U/mL) during the initial 20 min of nIR imaging resulted in decreased sensor fluorescence response to H_2O_2; mean ± SE (n = 4–6). (c) Sensitivity and reversibility of HeAptDNA-SWCNT sensors assessed by measuring the nIR fluorescence intensity changes after successive exposure to H_2O_2 at different concentrations from 1 to 10,000 μM; mean ± SE (n = 4); scale bar, 0.5 cm.

aptamers for a 600 nm long SWCNT) following a previously published method.[48]

The functionalization of SWCNTs with hemin leads to quenching of the sensor's nIR fluorescence in a concentration-dependent manner (Figure S3), and H_2O_2 further quenches the sensor fluorescence (Figure 2a). However, hemin also increases the relative H_2O_2 response (Figure 2c). Therefore, we evaluated the optimal ratio of hemin to aptamer DNA coated SWCNTs to improve the H_2O_2 sensing ability without compromising the photoluminescence readout of nanosensors for nIR remote detection. These *in vitro* experiments indicated that a ratio of 0.5 μM hemin to 2 nM HeAptDNA-SWCNTs is optimal for H_2O_2 sensing (Figure S3c,d). The corresponding sensor calibration curve (Figure 2c) shows sensitivity in the μM range and saturation around 100 μM in a time-dependent fashion (Figure 2d). The H_2O_2 sensing mechanism could be direct quenching of SWCNT fluorescence by H_2O_2 adsorption on the carbon nanotube surface as reported for certain functionalized SWCNTs.[49] However, without hemin functionalization, we observed no enhanced nIR fluorescence change. Therefore, it is more likely that hemin catalyzes a Fenton-like reaction of H_2O_2 to reactive hydroxyl radicals that quench SWCNT fluorescence in a similar fashion to the reaction with protons.[50] To evaluate the impact of other stress-related plant metabolites on HeAptDNA-SWCNT sensing ability, selectivity tests were performed against Ca^{2+}, sugar (sucrose and glucose), and plant hormone levels (methyl salicylate, abscisic acid, and jasmonate) (Figure 2e). Ca^{2+}, glucose, and sucrose regulate physiological and developmental responses to plant stress across diverse plant taxa.[23,51,52] Plant hormones such as abscisic acid are early signals of water stress,[53] jasmonate coordinates stress responses to salinity, freezing, drought, and wounding,[54] and methyl salicylate is involved in plant pathogen defense.[55] These stress-associated plant signaling molecules did not substantially affect the nIR fluorescence response of the HeAptDNA-SWCNTs. Additionally, the H_2O_2 sensing ability of HeAptDNA-SWCNTs in the presence of these stress-associated molecules was not impaired (Figure S4), highlighting their selectivity and capability for *in vivo* applications.

In Vivo Sensing of H_2O_2 by HeAptDNA-SWCNT Embedded in Plant Leaves. The SWCNT fluorescence in the nIR region falls into the tissue transparency window and low leaf autofluorescence range, making SWCNT-based sensors ideal for *in vivo* applications in plants. The nanosensors were embedded in leaves of *Arabidopsis* plants by a facile method of leaf lamina infusion using a needleless syringe, as performed previously in other plants.[18,19,42] Leaves were exposed to H_2O_2

https://dx.doi.org/10.1021/acs.nanolett.9b05159
Nano Lett. 2020, 20, 2432−2442

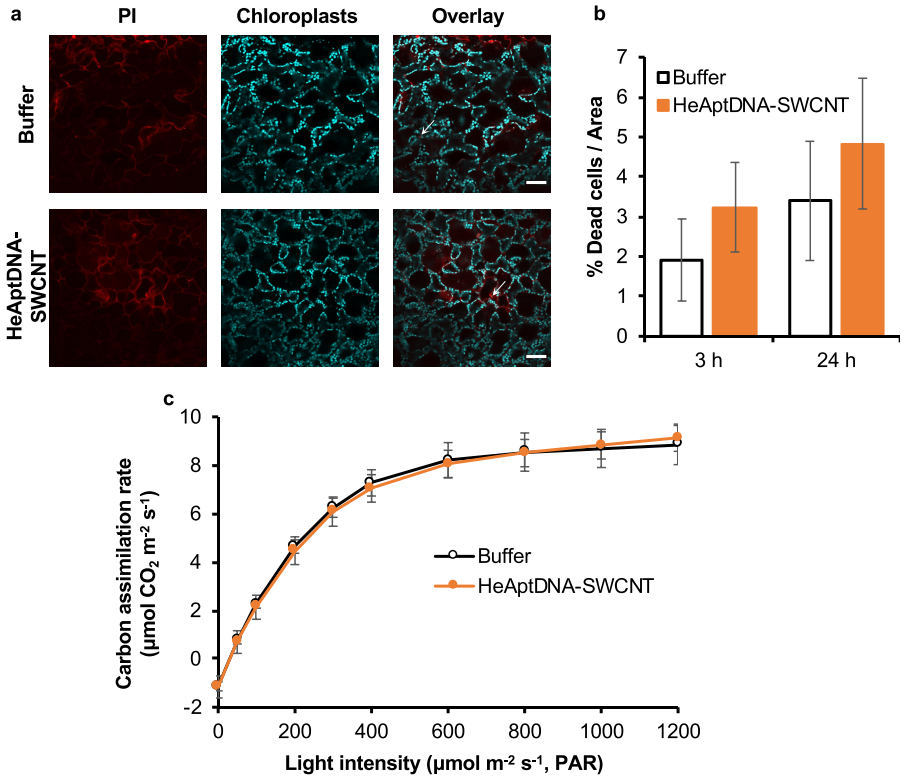

Figure 4. Biocompatibility of HeAptDNA-SWCNT sensors in plants. (a) Confocal microscopy images of *Arabidopsis* leaf mesophyll cells exposed to PI, a fluorescent dye that stains dead cells. Scale bar, 50 μm. (b) No significant differences in percentage of dead cells per area were observed between plants interfaced with HeAptDNA-SWCNT sensors and those treated with buffer (control) ($P < 0.05$, Student's t test); mean ± SE (n = 5). (c) Plant photosynthesis measured as leaf carbon assimilation rates at varied PAR levels was not impacted by HeAptDNA-SWCNT sensors compared to controls (buffer) ($P < 0.05$, Student's t test); mean ± SE (n = 6).

by direct application on the leaf surface, whereas plants treated with water instead of H_2O_2 were used as controls. Sensor fluorescence intensity changes in response to the leaf H_2O_2 exposure was monitored via its nIR fluorescence emission (Figure 3). The nIR imaging was performed using a remote nIR camera (Xeva-1.7-320 TE3) coupled to a 900 nm long-pass filter that allowed the detection of only nIR wavelengths from fluorescent SWCNTs, while deflecting the laser excitation (785 nm) and plant autofluorescence in the red and far-red range of the spectrum. A maximum emission intensity change (−14%) of HeAptDNA-SWCNT sensor was observed in *Arabidopsis* plants exposed to 100 μM H_2O_2 for 60 min (Figure 3a,b). After the removal of H_2O_2, the nIR emission intensity of HeAptDNA-SWCNT sensors was partially recovered (up to −6%), demonstrating that the sensor is reversible. The addition of a well-known H_2O_2 enzymatic scavenger (catalase, 1500 U/mL) to leaves before treatment with H_2O_2 resulted in a significant reduction of the sensor nIR fluorescence response to H_2O_2. Together, these results indicate that the sensor fluorescence quenching occurs in response to H_2O_2 in plants.

To investigate the sensitivity of HeAptDNA-SWCNT to H_2O_2 *in vivo*, we tested the sensor nIR fluorescence response in plant leaves to 1, 10, 100, 1000, and 10,000 μM H_2O_2 (Figure 3c, Video S1). The range of H_2O_2 concentrations from 1 to 100 μM is within the reported physiological range in plants.[17] The nIR emission intensity of HeAptDNA-SWCNT sensors was significantly reduced in response to 10 μM H_2O_2 down to −9.4% with further intensity decreases to −12.9% upon exposure to higher H_2O_2 concentrations. To our knowledge, this is the optical SWCNT sensor having the highest sensitivity to H_2O_2 (10 μM) *in vivo*, with an order of magnitude higher sensitivity than previous SWCNT sensor approaches using $(GT)_{15}$-SWCNTs.[19] After removal of H_2O_2 exposure at different concentrations, we observed the partial recovery of nIR emission intensity of HeAptDNA-SWCNT sensors, indicating their reversibility *in vivo* (Figure 3c). The HeAptDNA-SWCNT sensors in control leaves exposed to ddH_2O exhibited nonsignificant ($P > 0.05$) changes in nIR emission intensity (Figure 3c). These results demonstrate that HeAptDNA-SWCNTs are reversible sensors that report physiological levels of H_2O_2 in plants via nIR fluorescence signals to electronic devices.

The HeAptDNA-SWCNT sensors are also biocompatible within plants (Figure 4). We assessed the impact of embedded sensors in leaves by a cell viability assay using propidium iodide (PI), a fluorescent dye that stains dead plant cells.[56] Confocal images of leaf mesophyll cells stained with PI indicated no significant differences in the percentage of dead cells per leaf area for HeAptDNA-SWCNT sensor treated plants (4.8 ± 1.6%) compared with buffer control counterparts (3.2 ± 1.1%) (Figure 4a,b). Similarly, plant photosynthetic performance was not affected by HeAptDNA-SWCNT sensors (Figures 4c and S4). Both HeAptDNA-SWCNT and control plants showed similar leaf CO_2 assimilation rates over a wide range of light intensities (Figure 4c) and CO_2 concentrations (Figure S5). Thus, the high biocompatibility of these H_2O_2 optical nanosensors indicates minimal impact on plant health status.

https://dx.doi.org/10.1021/acs.nanolett.9b05159
Nano Lett. 2020, 20, 2432−2442

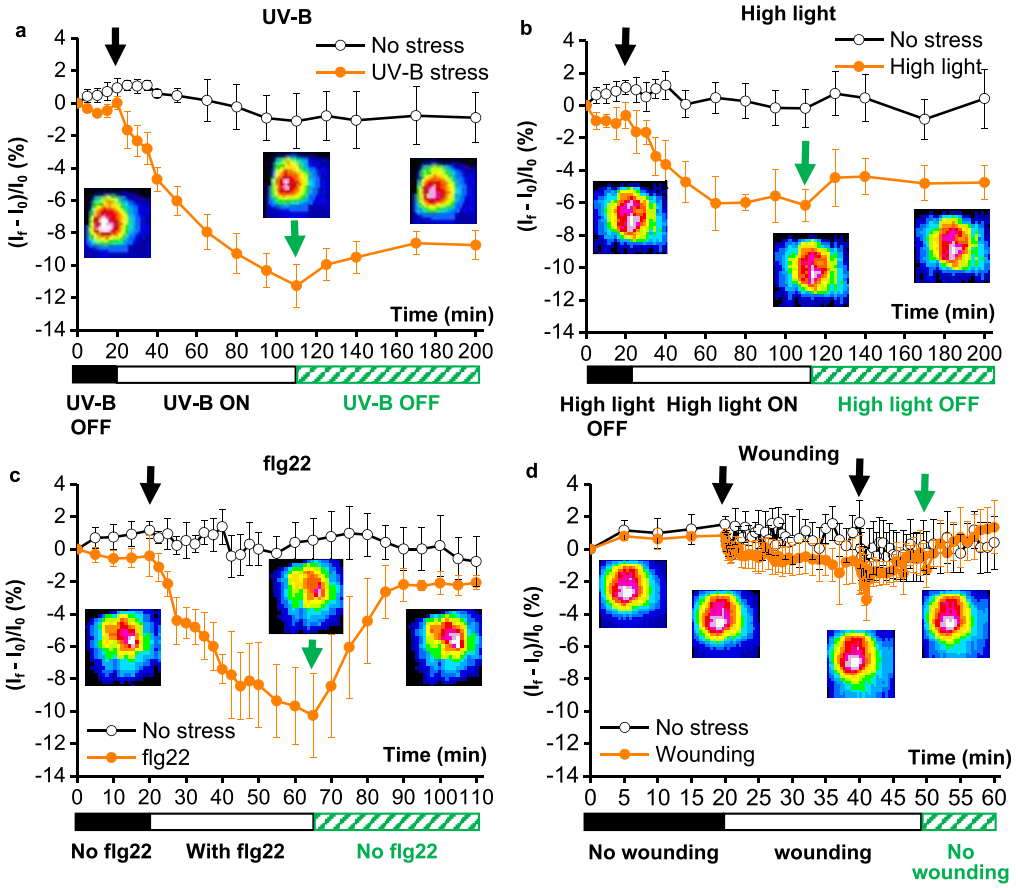

Figure 5. *In vivo* optical monitoring of plant health by H_2O_2 nanosensors. The nIR fluorescence intensity changes of HeAptDNA-SWCNT sensors in leaves (color map insets) report the onset of environmental stresses including UV-B, high light, and pathogen-associated peptide stress (flg22), but not leaf wounding. The sensor nIR fluorescence intensity decreases under (a) UV-B and (b) high light with a minor recovery of the initial fluorescence signal after the stress is removed. In contrast, (c) HeAptDNA-SWCNT nIR fluorescence quenching is followed by a strong recovery of emission intensity upon exposure and subsequent removal of flg22 peptide. (d) Leaf mechanical wounding did not impact sensor nIR fluorescence emission; mean ± SE (n = 4).

In Vivo Optical Monitoring of Plant Health under Stress. We observed a significant decrease in HeAptDNA-SWCNT nIR emission intensity from plants under UV-B (−11%), high light (−6%), and pathogen-related flg22 peptide (−10%) stresses relative to nonstress controls ($p < 0.05$) (Figure 5a−c). Rapid systemic ROS accumulation has been reported in plants in response to light stress, infection with bacterial pathogens, and mechanical wounding.[15] The flg22 peptide is used as a model for research on microbial pathogen induced response.[57] This peptide has a sequence derived from the flagellin N-terminus of the bacteria *Pseudomonas spp.* that is known to elicit immune responses in plants.[57] Leaf wounding by insects is also a common stress related to herbivore attack that negatively impacts plant growth.[58] However, mechanical wounding on leaves did not result in changes of the nIR emission intensity of HeAptDNA-SWCNT sensors ($p > 0.05$) (Figure 5d). The UV-B, high light, and flg22 treatments induced a decrease in nIR emission intensity of H_2O_2 sensors in plants within 60−120 min of stress exposure. The sensor fluorescence recovery after removal of the stress treatment varied from a strong change of −10% to −2% for flg22 and smaller changes of −11 to −9% for UV-B and −6% to −5% for high light, indicating different kinetics of the stress response to stress, especially for the microbial pathogen-related stress (flg22). Control plants under no stress conditions exhibited minor changes in sensor nIR emission intensity from 1.4 to −0.9% (Figure 5). Using a quantitative biochemical assay for H_2O_2, we measured a significant accumulation of leaf H_2O_2 concentration associated with the exposure of plants to UV-B, high light, and flg22 ($p < 0.05$), but not for leaf wounding compared to nonstress controls (Figure S6). The increase in leaf H_2O_2 levels from 30 to 60 μM relative to controls was within the sensor sensitivity (>10 μM H_2O_2). Together, these results demonstrate that HeAptDNA-SWCNT are able to monitor plant health in real-time by sensing H_2O_2 and report the onset of environmental stresses including UV-B, high light, and microbial pathogens.

Determining both the onset and type of plant stress would likely improve by multiplexing plant chemical signal sensing. Using chirality enriched SWCNTs, multiple spectrally encoded sensors could be imaged simultaneously[19,59] to allow other signaling molecules associated with plant health to be monitored in parallel. For example, this can be accomplished by interfacing plants with (6,5) and (7,6) enriched chirality SWCNT sensors having distinct fluorescence emission peaks in the nIR that can be recorded by hyperspectral imaging devices. For adequate performance in the field, the sensor durability is expected to span a growing season. SWCNT sensor lifetime has been reported in mammalian systems under laboratory conditions to be at least six months,[41] but needs to

https://dx.doi.org/10.1021/acs.nanolett.9b05159
Nano Lett. 2020, 20, 2432−2442

be assessed in plants under field conditions. The required spatial resolution of plants with nanosensors from sentinel individuals to groups of plants will depend on applications in plant phenotyping, urban or industrial agriculture, and microenvironment variations. Nanosensors with high sensitivity and selectivity, multiplexing and long lasting nonphotobleaching capabilities, and optical communication capabilities with existent nIR agricultural equipment are an emerging toolkit for chemical phenotyping and monitoring crop plant health.

Conclusions. Long-term sustainability of crop productivity will rely on precision agriculture, the use of data-driven technology in crop management, and improved plant phenotyping tools.[14,60,61] Plant nanobiotechnology promises transformative solutions to improve global agricultural security,[62−64] including the prospect of plant nanosensors able to communicate crop health status before stress symptoms manifest.[17] The HeAptDNA-SWCNT are selective sensors for H_2O_2, a fundamental plant signaling molecule associated with stress, and respond within the H_2O_2 plant physiological range (10−100 μM). The temporal dynamics of the nIR fluorescence quenching in response to plant stresses *in vivo* occurred in distinct time frames reaching a peak in intensity decrease at 60 min for pathogen-related stress (flg22) and 120 min for environmental stresses (UV-B and high light). Sensor reversibility *in vivo* was high after exposure to microbial pathogen-related stress (flg22) but not to environmental stresses (UV-B and high light). These differences in temporal patterns of fluorescence signal quenching and recovery opens opportunities for interpreting stress patterns and fingerprinting type and level of stress. It is known from other signaling processes in living systems that the spatiotemporal patterns of stress response might contain underlying information to pinpoint cell health status.[40] To analyze these complex spatiotemporal patterns, simulations and analysis require considering both sensor and stress kinetics.[65]

One advantage of SWCNT sensors is that they can be delivered through the leaf lamina on selected leaves or individuals using a needleless syringe, a simple, controlled, and practical nanoparticle foliar delivery method.[19,42] SWCNT can become kinetically trapped within plant cell and organelle lipid bilayers.[18,66,67] Thus, we expect that SWCNT translocation outside of leaves through the vascular tissue would be limited. Size and surface coating modifications can be tailored to localize nanoparticles in plant subcellular compartments,[67] which could allow more efficient delivery into specific leaf cells and organelles (e.g., stomatal guard cells, chloroplasts, and extracellular space). SWCNTs have also been functionalized with nanobodies as recognition units to bind to specific locations in organisms.[68] Such an approach combined with the H_2O_2 sensing demonstrated in this study could enable localization of nanosensors to specific compartments in plants. Overall, our results indicate that SWCNT-based nIR fluorescent nanosensors for H_2O_2 are able to report plant stress status remotely to macroscopic imaging devices. This nanobiotechnology-based approach provides a powerful sensing tool that can be translated to crop plant species for a more sustainable nano-enabled agriculture.

Methods. *Plant Growth.* *Arabidopsis thaliana* (Columbia 0) plants 4−5 weeks old were used in this study. Seeds were sown in standard soil mix (Sunshine, LC1 mix) filled pots (2 × 2 in., 32 inserts). One week after seed germination, only one seedling was kept in each pot. Plants were grown in an Adaptis 1000 growth chamber (Conviron). The growth chamber settings were set at 200 μmol m^{-2} s^{-1} photosynthetic active radiation (PAR), 24 ± 1 °C and 21 ± 1 °C at day and night times, respectively, 70% relative humidity, and 14h/10 h day/night regime. Plants were hand watered with deionized water twice per week.

Synthesis of Hemin Complexed Aptamer DNA-SWNCT (HeAptDNA-SWCNT). Hemin complexed HeAptDNA-SWCNT were synthesized by mixing 125 μL, 1 mg/mL (6,5) chirality enriched SWCNTs (Sigma-Aldrich, product no. 773735, in 10 mM *N*-[Tris(hydroxymethyl)methyl]-2-aminoethanesulfonic acid (TES), pH 7.0) with 125 μL, 2 mg/mL ssDNA (5′-AGTGTGAAATATCTAAACTAAATGTGGAGGGTGGGACGGGAAGAAGTTTATTTTTCACACT-3′, in 10 mM TES, pH 7.0) in a 1.5 mL eppendorf tube. After pipetting for 5 times, the mixture was tip sonicated (15 min, 30% Amplitude, Fisher Scientific Model 120 Sonic Dismembrator) in an ice bath. The sonicated mixture was then centrifuged for 60 min, 16,000*g*, at ambient temperature (two times). The supernatant was then transferred to a Vivaspin 500 MWCO (molecular weight cut off) filter (100,000 Da cutoff) and mixed with 500 μL of TES buffer, followed by centrifugation at 15,000*g* to remove excess ssDNA (3 times washing). Centrifugation cycles of 6−10 min allowed the mixture to be concentrated to 25 μL in the filter. After the washing steps, the purified samples were redispersed via tip sonication for 30 s (30% Amplitude, Fisher Scientific Model 120 Sonic Dismembrator). The sonicated mixture was centrifuged twice for 90 min at 16,000*g* and ambient temperature. The supernatant was collected in a new 1.5 mL eppendorf tube, and the concentration of this sample was determined by measuring the absorbance at 991 nm with a Cary 500 UV−vis/nIR spectrophotometer. The absorbance was used to calculate the SWCNT molar concentration by following a previously published protocol.[48] The concentrations used for *in vivo* experiments were 8 μM hemin and 16 nM aptamer DNA-SWCNTs. The synthesized hemin complexed aptamer DNA-SWCNT was stored at ambient temperature until further use.

In Vitro Characterization of HeAptDNA-SWCNT Sensor. UV-vis-nIR absorption spectroscopy was performed with a JASCO V-670 device acquiring a spectral range from 400 to 1350 nm in 0.2 nm steps. Fitting of absorbance spectra was performed as reported previously,[59] based on an approach from Pfohl et al.[69] The nIR fluorescence spectra were recorded with a Shamrock 193i spectrometer (Andor Technology Ltd., Belfast, Northern Ireland) connected to an IX53 microscope (Olympus, Tokyo, Japan). Excitation was performed with a gem 561 laser (Laser Quantum, Stockport, UK). 2D excitation−emission spectra were recorded with an monochromatic light source (MSH150; LSE341 light source, LOT-Quantum Design GmbH, Darmstadt, Germany). HiPco-SWCNTs (NanoIntegris HiPco Raw SWCNTs) were coated with HeAptDNA to determine the optimal SWCNT chirality for hemin complexation. For analyte-dependent nIR fluorescence response measurements, 180 μL of 2 nM HeAptDNA-SWCNT was placed in a 96-well plate and mixed with 20 μL of analyte at the desired concentration. The response of HeAptDNA-SWCNT to different H_2O_2 concentrations within 0.2−1.5 μM hemin concentration range was recorded from 0 to 40 min to analyze the sensors kinetic fluorescence response. Selectivity analysis of sensors was performed against plant molecules associated stress within

https://dx.doi.org/10.1021/acs.nanolett.9b05159
Nano Lett. 2020, 20, 2432−2442

the reported plant physiological range[17] by recording *in vitro* responses to nIR fluorescence intensity of the HeAptDNA-(6,5)-SWCNT spectra.

Nanosensor Delivery into Plant Leaves. A detailed protocol for leaf lamina infiltration of nanoparticles is given in Wu et al.[70] Briefly, selected leaf regions were slowly infiltrated with ~20 μL HeAptDNA-SWCNT (16 nM HeAptDNA-SWCNT, 8 μM hemin, in TES buffer) solution through the leaf abaxial (lower) side by gently pressing the tip of the syringe (1 mL NORM-JECT) against the leaf lamina. Kimwipes (Kimtech Science) were used to remove the excess nanoparticle solution on the leaf surface. The plants interfaced with the nanosensors were kept on the bench under room light (10−15 μmol m^{-2} s^{-1}) and ambient temperature at least 3 h for acclimation and incubation.

In Vivo Remote Imaging of HeAptDNA-SWCNT nIR Fluorescence Emission. A flat intact leaf of *Arabidopsis* plants (Col-0, 4−5 weeks old) grown in pots (2 × 2 in.) was infused with HeAptDNA-SWCNT. After incubation and adaption for at least 3 h on the lab bench, the pot and soil were carefully removed, while avoiding damage to the roots. The roots and remaining bounded soil were wrapped with cling wraps. Then the plant was laid down on a lab bench, and the flat leaf interfaced with HeAptDNA-SWCNT was immobilized on top of a laser safety screen (TPS5, THORLABS, USA) by using black tape without damaging the leaf. For nIR imaging of H_2O_2 nanosensors in leaves, a 785 nm laser (IBeam Smart, TOPTICA Photonics, Germany) and Xenics nIR camera (XEVA-CL-1.7-320, Xenics, Belgium) were used. The nIR laser was expanded by a plano-concave lens (N-BK7, Ø1/2″, THORLABS, USA) to a larger area on the plant leaf. The laser output was set at 250 mW. The Xenics nIR camera frame rate (up to 100 fps) was set to 2 fps. The camera was cooled below −40 °C. The distance between the nIR camera and the leaf was set to 70 cm, and the angle between the leaf surface and the line pointing from the camera to the leaf was about 75°.

To assess the *in vivo* sensing of H_2O_2 by HeAptDNA-SWCNT sensors, a 100 μL solution of different concentrations of H_2O_2 (30%, Thermo Fisher) was added on the adaxial (upper) leaf surface and removed during the nIR imaging for each time point. To facilitate diffusion of the H_2O_2 solution into the leaf, small holes were made on the leaf region infiltrated with HeAptDNA-SWCNT using the tip of fine forceps (Excelta 5SASE, Thermo Fisher), followed by 3 h acclimation to minimize impact of physical damage. During nIR imaging of nanosensors, plants were kept under room light conditions to prevent stomatal fully closure. For assessing the sensor nIR intensity changes in response to 100 μM H_2O_2, background images were recorded (0−20 min), then 100 μM H_2O_2 was added topically to the adaxial leaf surface (20−80 min), followed by removal of H_2O_2 (80−140 min). In addition, a H_2O_2 scavenging treatment was performed by adding 100 μL of catalase (1500 U/mL) on the adaxial side of the leaf surface. Images of nIR background were recorded (0−20 min) before removing catalase and adding 100 μM H_2O_2(20−80 min), followed by removal of H_2O_2 (80−140 min). The catalase or H_2O_2 solutions were removed before recording nIR images and re-added afterward. For assessing the sensitivity and reversibility of the sensors, the leaf nIR background was recorded (0−20 min), followed by applications of H_2O_2 at concentrations of 1 (20−50 min), 10 (95−125 min), 100 (170−200 min), 1000 (245−275 min), and 10,000 (320−350 min) μM H_2O_2, and removal of the applied H_2O_2 (50−95 min, 125−170 min, 200−245 min, and 350−395 min).

Plant stress treatments for UV-B, high light, flg22, and leaf wounding proceeded as follows: UV-B stress was induced in plants using a 365 nm UV lamp (3UV-38 UV lamp, UVP, LLC). High-light stress was generated by exposing leaves to ~1800 μmol m^{-2} s^{-1} of photosynthetic active radiation using a blue and red LED (light-emitting diode) (GFS 3000 gas analyzer, Walz, Germany). Images of nIR background (0−20 min) were recorded before turning UV or LED light stress on (20−110 min), followed by light stress off (110−200 min). Microbial pathogen stress was simulated using a 10 μM flg22 peptide (Genscript, dissolved in molecular grade water). Flg22 is a highly conserved 22 amino acid peptide from a bacterial flagellin which is well-known to induce microbial pathogen defense response in plants.[57] A 100 μL flg22 peptide solution (10 μM) was added on the adaxial (top) side of the leaf and removed during each measuring time point. The diffusion of the solution into the leaf was increased by minor holes made on the HeAptDNA-SWCNT region by using the tip of fine forceps and allowing 3 h acclimation after making minor holes to minimize the side effects due to the physical damage. During imaging, plants were kept under room light conditions to prevent stomatal closure. Images of nIR background (0−20 min) were recorded before exposing leaves to flg22 (20−65 min), followed by removal of flg22 (65−110 min). Plant wounding stress was induced by a dissecting needle (diameter, 1 mm) and successive punctures on the adaxial side of the leaf lamina approximately 2 cm away from the location of the sensors. Images of nIR background were recorded (0−20 min), followed by a first wounding event (20 min), then multiple wounding events (40−50 min), and no wounding afterward (50−60 min).

nIR Image Analysis. Snapshots of nIR images of nanosensors embedded in leaves collected by the nIR camera were analyzed with ImageJ. For plotting the HeAptDNA-SWCNT nIR intensity changes in plants under stress, the images from each biological replicate were converted into stacks. A leaf region with the HeAptDNA-SWCNT was selected for analysis of average nIR fluorescence intensity over time. SWCNT nIR intensity images were plotted by converting them from RGB (red, green, blue) mode to 32-bit format with ImageJ. Then, a 16-color LUT format was applied to highlight the differences of HeAptDNA-SWCNT intensity.

Leaf H_2O_2 Content. A quantitative peroxide assay kit (Pierce, Thermo Scientific, USA) was used to measure the concentration of H_2O_2 in leaves as reported previously with modifications.[71] Plants were exposed to UV-B light (365 nm, 90 min), high light (1800 μmol m^{-2} s^{-1} of photosynthetic active radiation, 90 min), flg22 peptide (10 μM, 60 min), leaf wounding as described above, and no stress (controls). Leaf disks were harvested after plant stress and control treatments using a 12 mm cork borer, weighed immediately in a microbalance (ML802E, Mettler Toledo), and frozen into liquid nitrogen (in less than 1 min). Samples were then grinded in 0.5 mL of DI (deionized) water using a prechilled mortar and pestle. Ground samples in DI water were transferred to a microtube (0.5 mL) and centrifuged at 13,000 rpm for 1 min. Then, 50 μL of supernatant was added to 500 μL of quantitative peroxide assay working reagent (0.25 mM ammonium ferrous sulfate, 100 mM sorbitol, 125 μM xylenol in 25 mM H_2SO_4). The absorbance of the diluted solution was measured in a UV−vis spectrophotometer (UV-

https://dx.doi.org/10.1021/acs.nanolett.9b05159
Nano Lett. 2020, 20, 2432−2442

2600, Shimadzu) after reaction at ambient temperature for 30 min to determine H_2O_2 concentration.

Biocompatibility Assays of HeAptDNA-SWCNT Sensors. Cell viability staining of the hemin complexed HeAptDNA-SWCNT infiltrated *Arabidopsis* (Col-0) leaves was performed using PI (PI, 0.1 mM, plant cell viability assay kit, PA0100, Sigma-Aldrich) as described in our previous work.[20] Briefly, *Arabidopsis* leaves were infiltrated with buffer control (10 mM TES, pH 7.0) and hemin complexed HeAptDNA-SWCNT (in 10 mM TES, pH 7.0). Then, at 3 h and 24 h, leaf discs were stained with PI for 30 min. The stained samples were then mounted on microscopy slides for confocal microscopy (Leica SP5) imaging as described in our previous publication.[70] Confocal imaging detection range was set at 590−640 nm for PI and 700−800 nm for chloroplasts under laser excitation of 488 nm.

Plant Photosynthesis. Photosynthesis (A) measurements were performed in plants infiltrated with buffer (controls) or HeAptDNA-SWCNT sensors as we have described previously.[72] Briefly, a portable Gas-Exchange and Fluorescence System (GFS-3000, WALZ, Effeltrich, Germany) was programmed to expose leaves to a progressive stepwise decrease in PAR (A−light curve) and CO_2(A−Ci curve). Measurements were conducted in a leaf gas exchange chamber at a temperature of 23 °C and 50% relative humidity. Photosynthetic response curves were built with 10 PAR levels from 0 to 1200 (0, 50, 100, 200, 300, 400, 600, 800, 1000, and 1200) μmol m^{-2} s^{-1} and eight CO_2 ambient levels from 50 to 800 (50, 100, 150, 250, 300, 500,600, and 800) ppm. Measurements of photosynthesis response to CO_2 were conducted before measurements of light curves at saturating light (1200 μmol m^{-2} s^{-1}). Infiltrated leaves with buffer and HeAptDNA-SWCNT sensors were allowed to acclimate at room temperature for 24 h before photosynthesis measurements.

Statistical analysis. All data from *in vivo* experiments were analyzed using SPSS 23.0. Comparisons were performed by independent samples *t*-test (two tailed) or one-way ANOVA based on Duncan's multiple range test (two tailed). *, **, and *** represent $P < 0.05$, $P < 0.01$, and $P < 0.001$, respectively. Different lowercase letters mean significance at $P < 0.05$.

■ ASSOCIATED CONTENT

Supporting Information

The Supporting Information is available free of charge at https://pubs.acs.org/doi/10.1021/acs.nanolett.9b05159.

Supplementary figures for *in vitro* characterization of H_2O_2 nanosensors, photosynthesis in plants interfaced with nanosensors, and leaf H_2O_2 content of plants under stress (PDF)

Video S1: Sensor nIR fluorescence response to H_2O_2 in Arabidopsis plant leaves. *In vivo* exposure and removal of H_2O_2 in leaves with embedded HeAptDNA-SWCNT results in quenching and partial recovery of the sensor nIR intensity (AVI)

■ AUTHOR INFORMATION

Corresponding Authors

Juan Pablo Giraldo − *Department of Botany and Plant Sciences, University of California, Riverside, California 92521, United States;* orcid.org/0000-0002-8400-8944; Email: juanpablo.giraldo@ucr.edu

Sebastian Kruss − *Institute of Physical Chemistry, Georg August University, Göttingen, 37077 Göttingen, Germany;* orcid.org/0000-0003-0638-9822; Email: skruss@uni-goettingen.de

Authors

Honghong Wu − *Department of Botany and Plant Sciences, University of California, Riverside, California 92521, United States; College of Plant Science and Technology, Huazhong Agricultural University, Wuhan 430070, China*

Robert Nißler − *Institute of Physical Chemistry, Georg August University, Göttingen, 37077 Göttingen, Germany*

Victoria Morris − *Department of Botany and Plant Sciences, University of California, Riverside, California 92521, United States*

Niklas Herrmann − *Institute of Physical Chemistry, Georg August University, Göttingen, 37077 Göttingen, Germany*

Peiguang Hu − *Department of Botany and Plant Sciences, University of California, Riverside, California 92521, United States;* orcid.org/0000-0002-9526-6295

Su-Ji Jeon − *Department of Botany and Plant Sciences, University of California, Riverside, California 92521, United States;* orcid.org/0000-0002-5917-8837

Complete contact information is available at: https://pubs.acs.org/10.1021/acs.nanolett.9b05159

Author Contributions

[‖]These authors contributed equally to this paper. J.P.G., S.K., H.W., and R.N. conceived and designed the study. H.W., R.N., N.H., P.H., V.M., and S.J. conducted the experiments. H.W., J.P.G, S.K., R.N., P.H., and S.J. analyzed the data. All authors contributed to writing the paper.

Notes

The authors declare no competing financial interest.

■ ACKNOWLEDGMENTS

We thank Mr. James Eckhardt for assistance with the development of the *in vivo* remote detection system for nIR nanosensors in plants. This work was supported by the National Science Foundation under grant no. 1817363 to J.P.G. and a grant by the Volkswagen Foundation to S.K.

■ REFERENCES

(1) Croppenstedt, A.; Cattaneo, A. et al. *Leveraging Food Systems for Inclusive Rural Transformation: The State of Food and Agriculture 2017*; Food and Agriculture Organization of the United Nations: Rome, Italy, 2017

(2) Piao, S.; Ciais, P.; Huang, Y.; Shen, Z.; Peng, S.; Li, J.; Zhou, L.; Liu, H.; Ma, Y.; Ding, Y.; et al. The Impacts of Climate Change on Water Resources and Agriculture in China. *Nature* **2010**, *467* (7311), 43−51.

(3) Chakraborty, S.; Newton, A. C. Climate Change, Plant Diseases and Food Security: An Overview: Climate Change and Food Security. *Plant Pathol.* **2011**, *60* (1), 2−14.

(4) Fisher, M. C.; Henk, D. A.; Briggs, C. J.; Brownstein, J. S.; Madoff, L. C.; McCraw, S. L.; Gurr, S. J. Emerging Fungal Threats to Animal, Plant and Ecosystem Health. *Nature* **2012**, *484* (7393), 186−194.

(5) Williamson, C. E.; Zepp, R. G.; Lucas, R. M.; Madronich, S.; Austin, A. T.; Ballaré, C. L.; Norval, M.; Sulzberger, B.; Bais, A. F.; McKenzie, R. L.; et al. Solar Ultraviolet Radiation in a Changing Climate. *Nat. Clim. Change* **2014**, *4* (6), 434−441.

(6) van Ittersum, M. K.; van Bussel, L. G. J.; Wolf, J.; Grassini, P.; van Wart, J.; Guilpart, N.; Claessens, L.; de Groot, H.; Wiebe, K.;

Mason-D'Croz, D.; et al. Can Sub-Saharan Africa Feed Itself? *Proc. Natl. Acad. Sci. U. S. A.* **2016**, *113* (52), 14964−14969.
(7) Paini, D. R.; Sheppard, A. W.; Cook, D. C.; De Barro, P. J.; Worner, S. P.; Thomas, M. B. Global Threat to Agriculture from Invasive Species. *Proc. Natl. Acad. Sci. U. S. A.* **2016**, *113* (27), 7575−7579.
(8) Dosio, A.; Mentaschi, L.; Fischer, E. M.; Wyser, K. Extreme Heat Waves under 1.5 Degrees C and 2 Degrees C Global Warming. *Environ. Res. Lett.* **2018**, *13* (5), 054006.
(9) Ummenhofer, C. C.; Meehl, G. A. Extreme Weather and Climate Events with Ecological Relevance: A Review. *Philos. Trans. R. Soc., B* **2017**, *372* (1723), 20160135.
(10) Pathak, T. B.; Maskey, M. L.; Dahlberg, J. A.; Kearns, F.; Bali, K. M.; Zaccaria, D. Climate Change Trends and Impacts on California Agriculture: A Detailed Review. *Agronomy* **2018**, *8* (3), 25.
(11) Velásquez, A. C.; Castroverde, C. D. M.; He, S. Y. Plant-Pathogen Warfare under Changing Climate Conditions. *Curr. Biol.* **2018**, *28* (10), R619−R634.
(12) Mahlein, A.-K. Plant Disease Detection by Imaging Sensors - Parallels and Specific Demands for Precision Agriculture and Plant Phenotyping. *Plant Dis.* **2016**, *100* (2), 241−251.
(13) Zarco-Tejada, P. J.; Camino, C.; Beck, P. S. A.; Calderon, R.; Hornero, A.; Hernández-Clemente, R.; Kattenborn, T.; Montes-Borrego, M.; Susca, L.; Morelli, M.; et al. Previsual Symptoms of Xylella Fastidiosa Infection Revealed in Spectral Plant-Trait Alterations. *Nat. Plants* **2018**, *4* (7), 432−439.
(14) Dhondt, S.; Wuyts, N.; Inzé, D. Cell to Whole-Plant Phenotyping: The Best Is yet to Come. *Trends Plant Sci.* **2013**, *18* (8), 428−439.
(15) Fichman, Y.; Miller, G.; Mittler, R. Whole-Plant Live Imaging of Reactive Oxygen Species. *Mol. Plant* **2019**, *12* (9), 1203−1210.
(16) Li, L.; Zhang, Q.; Huang, D. A Review of Imaging Techniques for Plant Phenotyping. *Sensors* **2014**, *14* (11), 20078−20111.
(17) Giraldo, J. P.; Wu, H.; Newkirk, G. M.; Kruss, S. Nanobiotechnology Approaches for Engineering Smart Plant Sensors. *Nat. Nanotechnol.* **2019**, *14* (6), 541.
(18) Giraldo, J. P.; Landry, M. P.; Faltermeier, S. M.; McNicholas, T. P.; Iverson, N. M.; Boghossian, A. A.; Reuel, N. F.; Hilmer, A. J.; Sen, F.; Brew, J. A.; et al. Plant Nanobionics Approach to Augment Photosynthesis and Biochemical Sensing. *Nat. Mater.* **2014**, *13* (4), 400−408.
(19) Giraldo, J. P.; Landry, M. P.; Kwak, S.-Y.; Jain, R. M.; Wong, M. H.; Iverson, N. M.; Ben-Naim, M.; Strano, M. S. A Ratiometric Sensor Using Single Chirality Near-Infrared Fluorescent Carbon Nanotubes: Application to In Vivo Monitoring. *Small* **2015**, *11* (32), 3973−3984.
(20) Li, J.; Wu, H.; Santana, I.; Fahlgren, M.; Giraldo, J. P. Standoff Optical Glucose Sensing in Photosynthetic Organisms by a Quantum Dot Fluorescent Probe. *ACS Appl. Mater. Interfaces* **2018**, *10* (34), 28279−28289.
(21) Bose, J.; Rodrigo-Moreno, A.; Shabala, S. ROS Homeostasis in Halophytes in the Context of Salinity Stress Tolerance. *J. Exp. Bot.* **2014**, *65* (5), 1241−1257.
(22) Choudhury, F. K.; Rivero, R. M.; Blumwald, E.; Mittler, R. Reactive Oxygen Species, Abiotic Stress and Stress Combination. *Plant J.* **2017**, *90*, 856−867.
(23) Zhu, J.-K. Abiotic Stress Signaling and Responses in Plants. *Cell* **2016**, *167* (2), 313−324.
(24) Torres, M. A.; Jones, J. D. G.; Dangl, J. L. Reactive Oxygen Species Signaling in Response to Pathogens. *Plant Physiol.* **2006**, *141* (2), 373−378.
(25) Kruss, S.; Hilmer, A. J.; Zhang, J.; Reuel, N. F.; Mu, B.; Strano, M. S. Carbon Nanotubes as Optical Biomedical Sensors. *Adv. Drug Delivery Rev.* **2013**, *65*, 1933−1950.
(26) Hong, G.; Diao, S.; Antaris, A. L.; Dai, H. Carbon Nanomaterials for Biological Imaging and Nanomedicinal Therapy. *Chem. Rev.* **2015**, *115* (19), 10816−10906.
(27) O'Connell, M. J.; Bachilo, S. M.; Huffman, C. B.; Moore, V. C.; Strano, M. S.; Haroz, E. H.; Rialon, K. L.; Boul, P. J.; Noon, W. H.; Kittrell, C.; et al. Band Gap Fluorescence from Individual Single-Walled Carbon Nanotubes. *Science* **2002**, *297* (5581), 593−596.
(28) Zheng, M.; Jagota, A.; Semke, E. D.; Diner, B. A.; McLean, R. S.; Lustig, S. R.; Richardson, R. E.; Tassi, N. G. DNA-Assisted Dispersion and Separation of Carbon Nanotubes. *Nat. Mater.* **2003**, *2* (5), 338−342.
(29) Welsher, K.; Liu, Z.; Sherlock, S. P.; Robinson, J. T.; Chen, Z.; Daranciang, D.; Dai, H. A Route to Brightly Fluorescent Carbon Nanotubes for near-Infrared Imaging in Mice. *Nat. Nanotechnol.* **2009**, *4* (11), 773−780.
(30) Zubkovs, V.; Schuergers, N.; Lambert, B.; Ahunbay, E.; Boghossian, A. A. Mediatorless, Reversible Optical Nanosensor Enabled through Enzymatic Pocket Doping. *Small* **2017**, *13* (42), 1701654.
(31) Polo, E.; Nitka, T. T.; Neubert, E.; Erpenbeck, L.; Vuković, L.; Kruss, S. Control of Integrin Affinity by Confining RGD Peptides on Fluorescent Carbon Nanotubes. *ACS Appl. Mater. Interfaces* **2018**, *10*, 17693−17703.
(32) Kruss, S.; Landry, M. P.; Vander Ende, E.; Lima, B. M. A.; Reuel, N. F.; Zhang, J.; Nelson, J.; Mu, B.; Hilmer, A.; Strano, M. Neurotransmitter Detection Using Corona Phase Molecular Recognition on Fluorescent Single-Walled Carbon Nanotube Sensors. *J. Am. Chem. Soc.* **2014**, *136* (2), 713−724.
(33) Mann, F. A.; Herrmann, N.; Meyer, D.; Kruss, S. Tuning Selectivity of Fluorescent Carbon Nanotube-Based Neurotransmitter Sensors. *Sensors* **2017**, *17* (7), 1521.
(34) Dinarvand, M.; Neubert, E.; Meyer, D.; Selvaggio, G.; Mann, F. A.; Erpenbeck, L.; Kruss, S. Near-Infrared Imaging of Serotonin Release from Cells with Fluorescent Nanosensors. *Nano Lett.* **2019**, *19* (9), 6604−6611.
(35) Bisker, G.; Dong, J.; Park, H. D.; Iverson, N. M.; Ahn, J.; Nelson, J. T.; Landry, M. P.; Kruss, S.; Strano, M. S. Protein-Targeted Corona Phase Molecular Recognition. *Nat. Commun.* **2016**, *7*, 10241.
(36) Harvey, J. D.; Jena, P. V.; Baker, H. A.; Zerze, G. H.; Williams, R. M.; Galassi, T. V.; Roxbury, D.; Mittal, J.; Heller, D. A. A Carbon Nanotube Reporter of microRNA Hybridization Events in Vivo. *Nature Biomedical Engineering* **2017**, *1*, 0041 DOI: 10.1038/s41551-017-0041.
(37) Jin, H.; Heller, D. A.; Kalbacova, M.; Kim, J.-H.; Zhang, J.; Boghossian, A. A.; Maheshri, N.; Strano, M. S. Detection of Single-Molecule H2O2 Signalling from Epidermal Growth Factor Receptor Using Fluorescent Single-Walled Carbon Nanotubes. *Nat. Nanotechnol.* **2010**, *5*, 302.
(38) Heller, D. A.; Jin, H.; Martinez, B. M.; Patel, D.; Miller, B. M.; Yeung, T. K.; Jena, P. V.; Höbartner, C.; Ha, T.; Silverman, S. K.; et al. Multimodal Optical Sensing and Analyte Specificity Using Single-Walled Carbon Nanotubes. *Nat. Nanotechnol.* **2009**, *4* (2), 114−120.
(39) Exposito-Rodriguez, M.; Laissue, P. P.; Yvon-Durocher, G.; Smirnoff, N.; Mullineaux, P. M. Photosynthesis-Dependent H 2 O 2 Transfer from Chloroplasts to Nuclei Provides a High-Light Signalling Mechanism. *Nat. Commun.* **2017**, *8* (1), 49.
(40) Kruss, S.; Salem, D. P.; Vuković, L.; Lima, B.; Vander Ende, E.; Boyden, E. S.; Strano, M. S. High-Resolution Imaging of Cellular Dopamine Efflux Using a Fluorescent Nanosensor Array. *Proc. Natl. Acad. Sci. U. S. A.* **2017**, *114* (8), 1789−1794.
(41) Iverson, N. M.; Barone, P. W.; Shandell, M.; Trudel, L. J.; Sen, S.; Sen, F.; Ivanov, V.; Atolia, E.; Farias, E.; McNicholas, T. P.; et al. In Vivo Biosensing via Tissue-Localizable near-Infrared-Fluorescent Single-Walled Carbon Nanotubes. *Nat. Nanotechnol.* **2013**, *8* (11), 873−880.
(42) Wong, M. H.; Giraldo, J. P.; Kwak, S.-Y.; Koman, V. B.; Sinclair, R.; Lew, T. T. S.; Bisker, G.; Liu, P.; Strano, M. S. Nitroaromatic Detection and Infrared Communication from Wild-Type Plants Using Plant Nanobionics. *Nat. Mater.* **2017**, *16*, 264.
(43) Pan, J.; Zhang, H.; Cha, T.-G.; Chen, H.; Choi, J. H. Multiplexed Optical Detection of Plasma Porphyrins Using DNA Aptamer-Functionalized Carbon Nanotubes. *Anal. Chem.* **2013**, *85*, 8391−8396.

https://dx.doi.org/10.1021/acs.nanolett.9b05159
Nano Lett. 2020, 20, 2432−2442

(44) Atsumi, H.; Belcher, A. M. DNA Origami and G-Quadruplex Hybrid Complexes Induce Size Control of Single-Walled Carbon Nanotubes via Biological Activation. *ACS Nano* **2018**, *12*, 7986−7995.
(45) Ensing, B.; Buda, F.; Baerends, E. J. Fenton-like Chemistry in Water: Oxidation Catalysis by Fe(III) and H2O2. *J. Phys. Chem. A* **2003**, *107*, 5722−5731.
(46) Enami, S.; Sakamoto, Y.; Colussi, A. J. Fenton Chemistry at Aqueous Interfaces. *Proc. Natl. Acad. Sci. U. S. A.* **2014**, *111* (2), 623−628.
(47) Traylor, T. G.; Xu, F. Mechanisms of Reactions of iron(III) Porphyrins with Hydrogen Peroxide and Hydroperoxides: Solvent and Solvent Isotope Effects. *J. Am. Chem. Soc.* **1990**, *112* (1), 178−186.
(48) Nißler, R.; Mann, F. A.; Chaturvedi, P.; Horlebein, J.; Meyer, D.; Vuković, L.; Kruss, S. Quantification of the Number of Adsorbed DNA Molecules on Single-Walled Carbon Nanotubes. *J. Phys. Chem. C* **2019**, *123*, 4837−4847.
(49) Crochet, J. J.; Duque, J. G.; Werner, J. H.; Doorn, S. K. Photoluminescence Imaging of Electronic-Impurity-Induced Exciton Quenching in Single-Walled Carbon Nanotubes. *Nat. Nanotechnol.* **2012**, *7* (2), 126−132.
(50) Cognet, L.; Tsyboulski, D. A.; Rocha, J.-D. R.; Doyle, C. D.; Tour, J. M.; Weisman, R. B. Stepwise Quenching of Exciton Fluorescence in Carbon Nanotubes by Single-Molecule Reactions. *Science* **2007**, *316* (5830), 1465−1468.
(51) Rolland, F.; Baena-Gonzalez, E.; Sheen, J. Sugar Sensing and Signaling in Plants: Conserved and Novel Mechanisms. *Annu. Rev. Plant Biol.* **2006**, *57*, 675−709.
(52) Tognetti, J. A.; Pontis, H. G.; Martínez-Noël, G. M. A. Sucrose Signaling in Plants: A World yet to Be Explored. *Plant Signaling Behav.* **2013**, *8* (3), No. e23316.
(53) Yoshida, T.; Mogami, J.; Yamaguchi-Shinozaki, K. ABA-Dependent and ABA-Independent Signaling in Response to Osmotic Stress in Plants. *Curr. Opin. Plant Biol.* **2014**, *21*, 133−139.
(54) Howe, G. A.; Major, I. T.; Koo, A. J. Modularity in Jasmonate Signaling for Multistress Resilience. *Annu. Rev. Plant Biol.* **2018**, *69*, 387−415.
(55) Lin, Y.; Qasim, M.; Hussain, M.; Akutse, K. S.; Avery, P. B.; Dash, C. K.; Wang, L. The Herbivore-Induced Plant Volatiles Methyl Salicylate and Menthol Positively affect Growth and Pathogenicity of Entomopathogenic Fungi. *Sci. Rep.* **2017**, *7*, 40494.
(56) Rounds, C. M.; Lubeck, E.; Hepler, P. K.; Winship, L. J. Propidium Iodide Competes with Ca2 to Label Pectin in Pollen Tubes and Arabidopsis Root Hairs. *Plant Physiol.* **2011**, *157*, 175−187.
(57) Albert, M. Peptides as Triggers of Plant Defence. *J. Exp. Bot.* **2013**, *64* (17), 5269−5279.
(58) Mitchell, C.; Brennan, R. M.; Graham, J.; Karley, A. J. Plant Defense against Herbivorous Pests: Exploiting Resistance and Tolerance Traits for Sustainable Crop Protection. *Front. Plant Sci.* **2016**, *7*, 1132.
(59) Nißler, R.; Mann, F. A.; Preiß, H.; Selvaggio, G.; Herrmann, N.; Kruss, S. Chirality Enriched Carbon Nanotubes with Tunable Wrapping via Corona Phase Exchange Purification (CPEP). *Nanoscale* **2019**, *11* (23), 11159−11166.
(60) Zhang, C.; Kovacs, J. M. The Application of Small Unmanned Aerial Systems for Precision Agriculture: A Review. *Precis. Agric.* **2012**, *13* (6), 693−712.
(61) Atzberger, C. Advances in Remote Sensing of Agriculture: Context Description, Existing Operational Monitoring Systems and Major Information Needs. *Remote Sensing* **2013**, *5* (2), 949−981.
(62) Lowry, G. V.; Avellan, A.; Gilbertson, L. M. Opportunities and Challenges for Nanotechnology in the Agri-Tech Revolution. *Nat. Nanotechnol.* **2019**, *14* (6), 517−522.
(63) Kah, M.; Tufenkji, N.; White, J. C. Nano-Enabled Strategies to Enhance Crop Nutrition and Protection. *Nat. Nanotechnol.* **2019**, *14* (6), 532−540.
(64) White, J. C.; Gardea-Torresdey, J. Achieving Food Security through the Very Small. *Nat. Nanotechnol.* **2018**, *13* (8), 627−629.
(65) Meyer, D.; Hagemann, A.; Kruss, S. Kinetic Requirements for Spatiotemporal Chemical Imaging with Fluorescent Nanosensors. *ACS Nano* **2017**, *11*, 4017−4027.
(66) Wong, M. H.; Misra, R.; Giraldo, J. P.; Kwak, S. Y.; Son, Y.; Landry, M. P.; Swan, J.; Blankschtein, D.; Strano, M. S. Lipid Exchange Envelope Penetration (LEEP) of Nanoparticles for Plant Engineering: A Universal Localization Mechanism. *Nano Lett.* **2016**, *16*, 1161−1172.
(67) Lew, T. T. S.; Wong, M. H.; Kwak, S.-Y.; Sinclair, R.; Koman, V. B.; Strano, M. S. Rational Design Principles for the Transport and Subcellular Distribution of Nanomaterials into Plant Protoplasts. *Small* **2018**, *14*, No. 1802086.
(68) Mann, F. A.; Lv, Z.; Großhans, J.; Opazo, F.; Kruss, S. Nanobody-Conjugated Nanotubes for Targeted Near-Infrared In Vivo Imaging and Sensing. *Angew. Chem., Int. Ed.* **2019**, *58* (33), 11469−11473.
(69) Pfohl, M.; Tune, D. D.; Graf, A.; Zaumseil, J.; Krupke, R.; Flavel, B. S. Fitting Single-Walled Carbon Nanotube Optical Spectra. *ACS Omega* **2017**, *2* (3), 1163−1171.
(70) Wu, H.; Tito, N.; Giraldo, J. P. Anionic Cerium Oxide Nanoparticles Protect Plant Photosynthesis from Abiotic Stress by Scavenging Reactive Oxygen Species. *ACS Nano* **2017**, *11* (11), 11283−11297.
(71) Cheeseman, J. M. Hydrogen Peroxide Concentrations in Leaves under Natural Conditions. *J. Exp. Bot.* **2006**, *57* (10), 2435−2444.
(72) Wu, H.; Shabala, L.; Shabala, S.; Giraldo, J. P. Hydroxyl Radical Scavenging by Cerium Oxide Nanoparticles Improves Arabidopsis Salinity Tolerance by Enhancing Leaf Mesophyll Potassium Retention. *Environ. Sci.: Nano* **2018**, *5*, 1567−1583.

https://dx.doi.org/10.1021/acs.nanolett.9b05159
Nano Lett. 2020, 20, 2432−2442